MDPI

Technical Note

Reimagining Prosthetic Control: A Novel Body-Powered Prosthetic System for Simultaneous Control and Actuation

Vikranth H. Nagaraja [ID], Jhonatan da Ponte Lopes [ID] and Jeroen H. M. Bergmann *[ID]

Natural Interaction Lab, Department of Engineering Science, Institute of Biomedical Engineering, University of Oxford, Parks Road, Oxford OX1 3PJ, UK; vikranth.harthikotenagaraja@eng.ox.ac.uk (V.H.N.); jhonatan.dapontelopes@eng.ox.ac.uk (J.d.P.L.)
* Correspondence: jeroen.bergmann@eng.ox.ac.uk

Abstract: Globally, the most popular upper-limb prostheses are powered by the human body. For body-powered (BP) upper-limb prostheses, control is provided by changing the tension of (Bowden) cables to open or close the terminal device. This technology has been around for centuries, and very few BP alternatives have been presented since. This paper introduces a new BP paradigm that can overcome certain limitations of the current cabled systems, such as a restricted operation space and user discomfort caused by the harness to which the cables are attached. A new breathing-powered system is introduced to give the user full control of the hand motion anywhere in space. Users can regulate their breathing, and this controllable airflow is then used to power a small Tesla turbine that can accurately control the prosthetic finger movements. The breathing-powered device provides a novel prosthetic option that can be used without limiting any of the user's body movements. Here we prove that it is feasible to produce a functional breathing-powered prosthetic hand and show the models behind it along with a preliminary demonstration. This work creates a step-change in the potential BP options available to patients in the future.

Keywords: assistive technologies; body-powered device; limb difference; paediatric users; Tesla turbine; upper limb

1. Introduction

There are over 40 million limb-deficient individuals worldwide, most of whom do not have access to any form of prosthetic care [1]. The World Health Organization (WHO) has estimated that among this population, upper-limb (UL) loss or absence accounts for about 16 % [2]. Global estimates for congenital UL differences vary widely and range from 4 to 5/10,000 to 1/100 live births [3]. Acquired UL amputations can be due to a wide variety of aetiologies, with the primary cause often being trauma. Unfortunately, most UL prosthetics currently available to patients are often neither affordable nor applicable in more challenging environments. The issue of appropriate prosthetics is even more pressing for children and adolescents, as there are fewer options available to them [4–6]. There is immense variability between and within countries regarding how children with UL differences are treated [7]. Active prostheses such as myoelectric devices are rarely fitted to the skeletally immature (this is especially true before the age of four) due to cost, weight, and/or muscle strength constraints [8]. Most children are, therefore, typically provided with a passive device or a body-powered (BP) prosthesis as their first active device [6,8–10]. These systems play a vital role in improving their gross motor development [10]. Passive devices have been generally associated with higher rejection rates in children because of a preference for function over cosmesis [5]. Providing suitable active devices to children and adolescents—and, consequently, improving their quality of life (QOL) as well as prosthetic outcomes in the long term—should thus be a priority.

The reported benefits of body-powered (BP) prostheses include silent action, lightweight, moderate cost, increased reliability, reduced training period, simple maintenance, proprioceptive feedback, and a simple operational mechanism that uses the body motions of the user to voluntary open or close the terminal device [11]. Furthermore, a voluntary closing BP prosthesis provides the user with extended physiological proprioception [12]. It extends the proprioceptive feedback to tools that users might engage with.

Various prosthetic options are available based on an individual's level of UL difference [13,14]. However, the most widely-used and affordable UL prosthesis across different settings and decades remains a Bowden cable-driven BP system [9,15–19]. The earliest recorded model of a BP prosthesis is the 'Ballif arm', which dates back to 1818 [20–22], making it now more than two centuries old. This purely mechanical technology still dominates much of the market despite the great efforts taken to offer the improved provision of artificial hands for the user population [18,19,23–25]. There has been little progress in developing new approaches specifically for powerand control of BP devices compared to their myoelectric counterparts [11,18,19]. As detailed earlier, BP prostheses have many advantages over externally-powered (EP) devices (e.g., myoelectric arms). However, despite these advantages, BP devices are rejected as frequently as EP devices for reasons like comfort (especially of the harness). The cost of even a standard (entry-level) BP device can be prohibitively expensive to own and maintain in low-resource settings. Moreover, BP prostheses usually require extensive fitting procedures from a high-skilled professional. Traditional BP devices rely on a harness system for their control that results in a restrictive operational workspace [26]. Unfortunately, current BP prostheses are also associated with higher rates of device repair and maintenance compared to other device types [27–29]. In addition, they often include cables and harnesses [30] that many children and female users find uncomfortable or cumbersome [31–33]. Users rejecting BP prostheses frequently describe the poor comfort and cosmesis associated with the traditional figure-of-eight and figure-of-nine harnesses [15,33].

Current BP prosthetics typically necessitate high operating forces [34–36], which could result in pain and fatigue during and/or after operation [33]. BP prostheses are reported to be mechanically inefficient [34,35,37] and offer a limited pinch force despite necessitating high cable operation forces from the user [34,35]. The high operation forces for BP prostheses contribute to their relatively high rejection rates [15]. Apart from fatigue and pain as primary drawbacks, high cable operation forces have also been found to deteriorate pinch force control accuracy in voluntary closing (VC) prostheses [38]. Notably, Hichert et al. [39] report that users of BP prostheses perceive and control low operation forces better than high forces. Consequently, their main advantage of offering feedback to the user is overshadowed, and the high operating forces negatively influence the comfort.

UL prostheses—and specifically BP devices—have generally witnessed poor outcomes, as the functional gain is limited compared to the disadvantages felt by the users [15,40–44]. UL prostheses' low success rates underscore the vast need for further improvements in this area [45–48]. In a large-scale epidemiological study, Atkins et al. [49] reported that users sought improvements in prosthetic control mechanisms, with the option to reduce the amount of visual attention needed. Ease of control and elimination of the harness altogether has remained a hope for BP device users [33,50]. According to a 2015 survey [51], participants generally still preferred novel techniques for UL prosthetic control that are not surgically invasive, wherein they expressed the highest interest in basic prosthesis features (e.g., opening and closing the hand slowly), compared to sophisticated features (e.g., touch sensation offered by some highly surgically-invasive techniques for bionic limbs) [52–55]. Choosing the path between invasive and non-invasive UL prosthetics has remained an ongoing topic for general discussion in the field [56]. BP prosthesis users' design priorities and needs have remained virtually unchanged for decades [33,44,49,50], and little attention has been given to broadening the design choices available to them. Recently, the "Self-Grasping Hand" was developed (for adults with hand absence) at the Delft University of Technology [57,58] to address the need for a purely mechanical device

that does not require harnessing. However, the Self-Grasping Hand is a passive-adjustable device that does not provide the user with continuous control over grasping movement compared to active UL prostheses. Besides, as opposed to an active prosthesis, most passive-adjustable devices require some involvement from the contralateral hand or the surrounding environment during the 'grasp' and 'release' phase. Another alternative is the "Wilmer Elbow Control", which is a harness-free, elbow-controlled BP prosthesis (that uses the elbow's flexion-extension movements as a control input instead of a traditional harness) [59,60]. However, the obvious downside to this approach is that the elbow's movement is coupled to the TD actuation. Hence, any unintended elbow motion leads to TD opening or closing, thereby restricting the user's desirable operational space. Efforts are still underway in the quest for a more appropriate or fit-for-purpose BP prosthesis for both adults and children [6,59,61–63].

Principally, one of the most significant challenges in this field has been the control of a UL prosthesis [43,64]. Identifying novel, intuitive, and non-invasive control options for UL prostheses is an ongoing topic of interest for researchers, academics, and clinicians alike [43,65–68]. The human body can generate a wide variety of control signals that could potentially be used to operate a prosthetic hand. Most practical control inputs typically originate from muscular activity around the arm and shoulder. The primary sources of control for BP prostheses are biomechanical. When body power is insufficient or undesirable, EP components may be utilised. The source of the "external power" comes from outside the human body. Contemporary versions are battery-powered electronic devices but can also rely on, for instance, pneumatic or hydraulic sources [16,18–20,46,69–71]. Despite its numerous benefits, this "external power" approach limits the operating time required for continuous use and increases the weight, complexity, safety requirements, and/or device cost. Furthermore, improvements in control are still sought [47]. This is an issue in particular for paediatric users or in low-resource settings. Alternatively, in a BP prosthesis, motion from the musculoskeletal (MSK) system is usually harnessed to power the technology. Still, conflicts in control can arise when the MSK system is both the power generator and the system being augmented/supplemented. Thus, an independent modality that can drive this kind of assistive technology could create a new robust alternative source for device power and control.

The exciting idea is to provide a novel customised BP device that allows the user to disconnect the positioning of the artificial hand in the user's workspace from the control and power requirements (which are currently imposed by the harness and cable). This implies that the user can freely place their prosthetic hand anywhere in space without it affecting the device's operation or function. This is particularly promising for UL-deficient children and adolescents, as their prosthetic operating space should not be limited as they grow and develop. Prosthesis use in children has been found to affect the development of their brain, as well as their motor control strategies [72–76]. This could have implications for long-term prosthetic outcomes. It is argued that a device powered and controlled by breathing input could expand the user options and address specific requirements that are difficult to meet with current BP prostheses. We can regulate our exhalation by forcing the diaphragm upward, and the controllable airflow can subsequently be used to power a small (custom-built and optimised) Tesla turbine [77], which can then help to achieve accurate control of the artificial hand. This breathing-powered device provides a patient-specific prosthetic option that can be used without limiting any of the user's body movements, compared to the traditional BP devices. This technical feasibility paper presents a novel type of BP prosthetic arm that relies on the user's respiratory system to power and control the TD. It introduces a breathing-powered prosthetic hand design comprising a purpose-built Tesla turbine and a transmission system suitable for paediatric users.

2. Materials and Methods

The methodology for this work consisted initially of developing mathematical models and virtual prototypes that could adequately describe the performance of the individual

components of the prosthesis. The design process started with determining a suitable turbine. The results from the turbine design were then used to design the transmission system. Finally, the TD was considered to accommodate the turbine/transmission assembly and provide key prosthetic device functionality. After the virtual prototyping phase, efforts were undertaken to make physical prototypes and subsequent preliminary real-world testing.

2.1. Turbine

There is a need to convert the user's breathing input into mechanical power, and a turbine is one of the means to achieve this requirement. The choice of the turbine can be narrowed down by considering two key aspects of the application. First, the operating fluid is not conventional, composed of moist air riddled with impurities, such as dust or small debris that might travel along the breathing tube. Hence, the operating fluid cannot be assumed homogeneous, as it might contain particulates that travel at high speed inside the turbine and can cause damage to the internal components. In addition, it is desirable to have the option of bidirectional operation of the turbine for control purposes, as it allows for an additional degree of freedom in the system without significantly increasing its complexity.

Conventional bladed turbines are, therefore, unsuitable for this application since the blades could be subjected to damage by the fluid's particulates at high speeds and due to their inherent unidirectionality. Based on a scan of the literature, a Tesla turbine—a bladeless centripetal flow turbine patented by Nikola Tesla in 1913—seemed to be the most suitable option that could meet the design requirements and constraints. The rotors of Tesla-type turbomachinery are composed of flat parallel co-rotating discs spaced along a central shaft. The inlet nozzle injects the fluid nearly tangentially into the rotor, where it passes through the narrow gaps between the discs, moving spirally towards a central exhaust port at each disc. Power is generated by the momentum exchange between the operating fluid and the discs' walls via a viscous drag force, resulting from the frictional behaviour of the fluid's boundary layer close to the walls due to the relative velocity between the disc and fluid.

There are several advantages to employing a Tesla turbine in detriment to a conventional bladed design. Because of their simple design, Tesla turbomachineries are easy to manufacture, maintain, and balance, which results in a low-cost, inexpensive turbine. In addition, the lack of blades and its self-cleaning nature (due to the centrifugal force field on the blades) enables it to generate power from various working media, such as Newtonian and non-Newtonian fluids, mixed fluids, and particle-laden two-phase flows [78]. Furthermore, the same rotor can be operated in clockwise or anticlockwise directions. Finally, it boasts a high power-to-weight ratio and low noise level [79]. These qualities make the Tesla turbine a suitable candidate for power extraction in biomedical applications [80,81].

While rotor efficiencies can be very high in Tesla turbines (up to 99 %), the inlet and outlet nozzles are necessarily long and inefficient, introducing inherent losses as fluid flows through them [82]. As a result, actual Tesla turbomachines have efficiencies much lower than theoretically expected. Experimental investigations show that their actual efficiencies are between 14.63 and 35.5 % [83–87]. More recently, Lemma et al. [88] reported a maximum efficiency lower than 25 % in their turbines. Considerations of design parameters are therefore essential for this early-stage research.

2.2. Tesla Turbine Model

Guha and Sengupta [89] (see also [82]) present a thorough discussion on current and previous mathematical models for predicting performance of Tesla turbines, which are often limited by either low mathematical accuracy [90], inaccurate physical modelling [83,91,92], lack of experimental validation [93], or oversimplified assumptions [94].

In order to overcome these limitations, Sengupta and Guha's [79] developed an analytical model for the fluid flow in the gap between two discs, which was verified against

Computational Fluid Dynamics (CFD) models and experimental data [79,88]. It solves the Navier–Stokes equations for the flow between two discs, assuming that [79]: the fluid is Newtonian with constant properties, the flow is steady and axisymmetric, the axial velocity is negligible compared to radial and tangential velocities, radial gradients are smaller than the axial gradients, body forces along r and θ directions are negligible, the flow is laminar, and the flow characteristics between any two discs of the rotor are the same. This model was chosen to produce a virtual prototype of the turbine and assess the order of magnitude of torque and power produced.

The flow enters the disc gap at a radius r_i and exits it at a central outlet at $r = r_o$. The gap is given by b (Figure 1). The fluid has a density ρ and a kinematic viscosity μ ($\nu = \mu/\rho$). The inlet of the turbine is a circular plenum chamber (vaneless diffuser) [78,88], which converts the radial velocity to tangential velocity. At the inlet of the rotor, the area-averaged radial and tangential components of the fluid velocity are given as $\bar{V}_{r,i}$ and $\bar{V}_{\theta,i}$, and their distributions along the rotor are given as $V_{r,i}(r,z)$ and $V_{\theta,i}(r,z)$. The rotor spins at a radial velocity Ω.
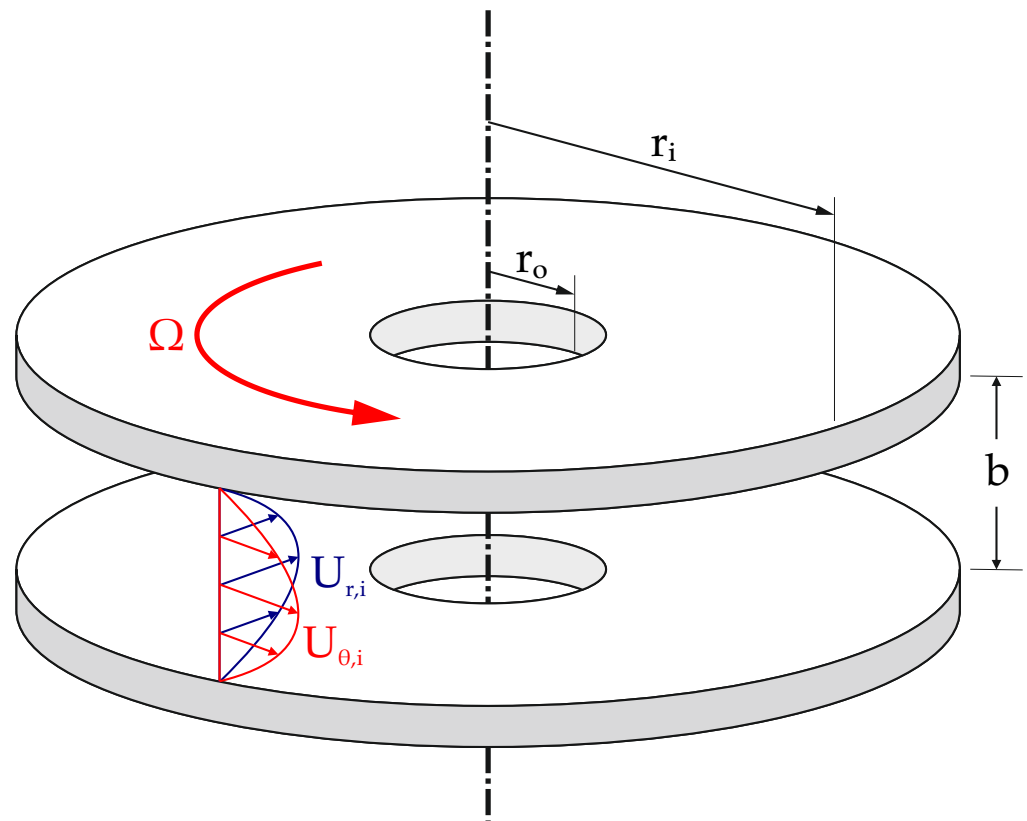

Figure 1. Analytical model for the fluid flow of a Tesla turbine design. The flow enters at radius r_i and exits the central outlet at r_o. The gap is given by b. Ω is the rotational speed of the disc and the absolute velocity of the fluid is given by U, with the subscript of θ reflecting the azimuthal direction in cylindrical coordinate system.

This model predicts that torque produced by a rotor consisting of n_d discs is given as:

$$\Gamma = \frac{24 n_d \pi \mu \bar{V}_{\theta,i} \, r_i^2}{b} \left[C_3(1 - R_o^2) - \frac{C_4}{C_1} \right.$$

$$\left. \times \left\{ \exp\left(-\frac{C_1}{2} \right) - \exp\left(-\frac{C_1 R_o^2}{2} \right) \right\} \right], \tag{1}$$

where

$$R_o = \frac{r_o}{r_i} \tag{2}$$

$$\phi_o = \frac{\bar{V}_{r,i}}{\Omega \, r_i} \tag{3}$$

$$\gamma = \frac{\bar{V}_{\theta,i} + \Omega \, r_i}{\Omega \, r_i} \tag{4}$$

$$C_1 = \frac{10\nu}{\phi_o \, \Omega \, b^2} \tag{5}$$

$$C_2 = \frac{-10}{6(\gamma - 1)} \tag{6}$$

$$C_3 = \frac{C_2}{C_1} \tag{7}$$

$$C_4 = (1 - C_3) \, \exp\left[\frac{C_1}{2}\right]. \tag{8}$$

The theoretical ideal power output is given by:

$$\dot{W} = \Gamma \, \Omega. \tag{9}$$

A limitation of Equations (1) and (9) is that their inputs are related to the flow conditions inside the turbine (at the inlet of the rotor), which can be difficult to estimate. Therefore, it is necessary to construct a model of the inlet nozzle plenum chamber to link the power and torque production to the breathing inputs.

Conservation of mass in the plenum chamber gives us $\bar{V}_{r,i}$ as:

$$\bar{V}_{r,i} = \frac{\dot{m}}{\rho A_c} = \frac{Q}{A_c}, \tag{10}$$

where $\dot{m}$ and Q are the mass and volumetric flow rates through the rotor, respectively, and A_c is the wetted area of the rotor inlet (cross-sectional area of the gaps where the working fluid passes through), given by:

$$A_c = 2\pi \, r_i \, b \, (n_d - 1). \tag{11}$$

Since the plenum chamber can be thought of as a vaneless diffuser, we disregarded frictional losses in this component and considered that the angular momentum must be conserved, i.e.,:

$$\bar{V}_{\theta,i} = \bar{V}_{\theta,inlet} \frac{r_i}{r_{plenum}}, \tag{12}$$

where $\bar{V}_{\theta,inlet}$ represents the area-averaged tangential velocity at the inlet of the plenum chamber and r_{plenum} represents its radius.

2.3. Transmission

Several design requirements and constraints must be considered to select the optimal transmission mechanism whilst maintaining a small overall size and weight of a prosthetic TD. Minimal friction and inertia—along with virtually no backlash—are particularly important if fingers are required to perform tasks involving dexterous manipulation. Indeed, nonlinear effects due to friction or backlash could make it difficult or impossible to control the movements accurately. Compared to alternatives (e.g., tendon/sheath, linkages and cams, flat bends and belt), gear trains are more suited for our application as they offer the best stiffness properties to the transmission, are less noisy, require low maintenance, are reliable, and allow bidirectional 'push and pull' control of the joint [69]. This bidirectional

feature is exceptionally suited to be compatible with both directions of rotation of the Tesla turbine rotor. Nevertheless, it should be noted that gears' employment can substantially increase the weight, complexity, and sometimes even hand dimensions [69].

An actuator technology should be chosen such that the largest 'motor-gearhead' combination will fit within the physical constraints of the mechanism being designed [16]. Based on a literature review of prosthetic hands for children, the output requirements of the transmission were 9.81 N (1 kg) of grip force [61] and 1 s of open/close time [25,95,96]. The input from the Tesla turbine to the transmission system—based on optimisations and virtual prototyping results—was 2.5 Nmm at 2500 RPM. Clearly, the Tesla turbine here produces excessive speed and insufficient torque for prosthetic applications. As a result, drive reductions were considered necessary to reduce the speed and increase the torque provided by the actuator [16]. The objective here is to maximise performance by optimising output speed and torque to attain physiological speeds and torques. Therefore, a transmission was designed using a series of meshing (simple and compound) spur gears and a worm drive at the last stage to obtain the required speed, torque, and self-locking (Table 1). Spur gears were mainly chosen as they provide one of the highest efficiencies (in the range of 94–98%).

The theoretical gear output torque is given by (Equation (13)):

$$M_0 = M_i r \eta \tag{13}$$

where M_0 represents the output torque (in Nm), M_i represents the input torque (in Nm), r represents the gear transmission ratio, and η represents the gear efficiency (in %).

Table 1. Transmission gear train details.

Gear Label	Shaft Type	Gear Type	Teeth/Start (For Worm)	Input Torque, M_i (In Nm)	Gear Transmission Ratio, r	Gear Efficiency, η	Output Torque, M_o (In Nm)	Rotations per min, (In RPM)
Gear A	Simple (Input)	Spur	10	0.0025	-	-	0.0025	2500
Gear B	Compound	Spur	30	0.0025	3:1	0.95	0.0071	833.3
Gear C		Spur	10	0.0071	1:1	1	0.0071	833.3
Gear D	Compound	Spur	40	0.0071	4:1	0.95	0.0271	208.3
Gear E		Spur	10	0.0271	1:1	1	0.0271	208.3
Gear F	Compound	Spur	60	0.0271	6:1	0.95	0.1543	34.7
Gear G		Worm	Single	0.1543	1:1	1	0.1543	34.7
Gear H	Simple (Output)	Worm wheel	10	0.1543	10:1	0.85	1.3118	3.5

Prosthetic hand function strongly depends on actuator performance, which subsequently affects the entire system's performance [69]. Thus, one important consideration concerns the need for non-back-drivable mechanisms (NBDMs). A transmission is termed non-back-drivable when motion can only be transmitted from the input to the output axis, not vice versa. In robotics and prosthetics, mostly lead screw and worm drives have been employed as non-back-drivable gearing between the actuator and the fingers or grippers [69,97,98]. Hence, our gearbox for the prosthesis was designed such that a worm drive at the final stage offers self-locking and acts as an NBDM. Another rationale for choosing a worm drive is that it provides a high gear ratio in a small volume. However, the efficiency of a worm drive is inversely related to the gear ratio. Consequently, a smaller gear ratio of 10:1 was chosen to provide higher efficiency at this stage. Besides, the number of starts on a worm gear is one of the factors that influence the self-locking ability, i.e., it is easier to self-lock when the number of starts becomes smaller. Consequently, a single-start worm drive was chosen in the transmission design.

Compared to other locking options available [97], a worm drive possesses several desired properties that can be deemed compatible with the breathing-powered, Tesla turbine-based prosthesis. If the stiffness of the frame and the fingers are sufficiently high, a worm drive allows the actuated finger to passively maintain a grip force without continued

powering of the Tesla turbine, thus minimising the requirement of continuous user input. In prosthetics, non-back-drivability is also vital for safety reasons. If a user stops powering the Tesla turbine, then it should not cause the (potentially dangerous) release of a grasped object [98]. The chosen locking type is passive, offers friction-based locking (i.e., due to shear friction), and avoids energy losses.

3. Results

Mathematical models and virtual prototypes were used in the initial phase of the design process. A virtual prototype of the turbine was constructed, according to the previously described methods, to allow fast iteration over key design parameters.

3.1. Turbine

The overall design of the turbine is shown in Figure 2, consisting of a rotor with N discs, a plenum chamber and an inlet tube. A plenum chamber was incorporated as the turbine's inlet component to maximise the conversion of radial velocity into tangential velocity, which significantly improves the rotor's efficiency [78,88].
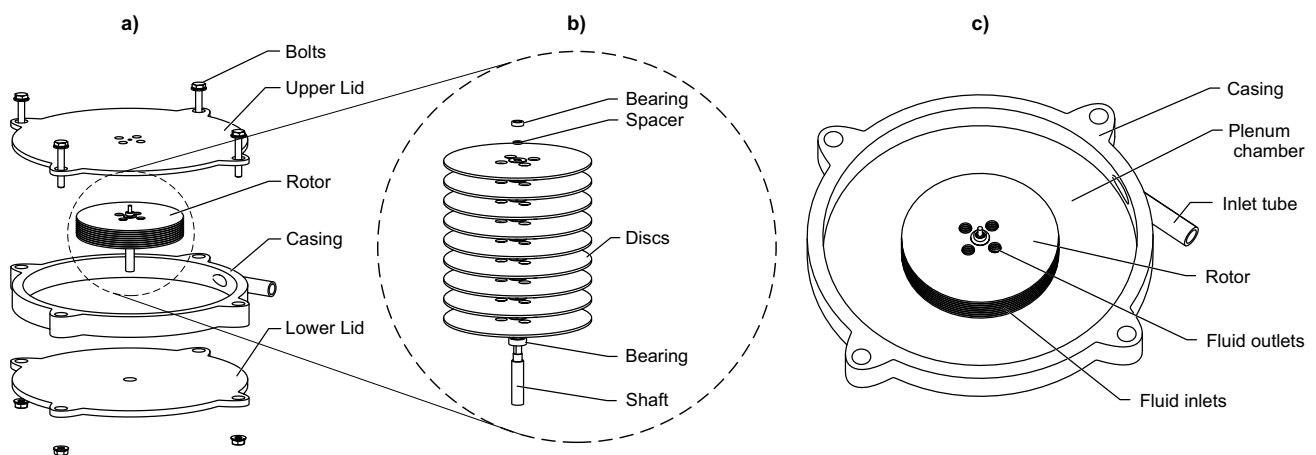

Figure 2. Tesla turbine design. (**a**) Top level components. (**b**) Detail view of the rotor. (**c**) Fluid regions.
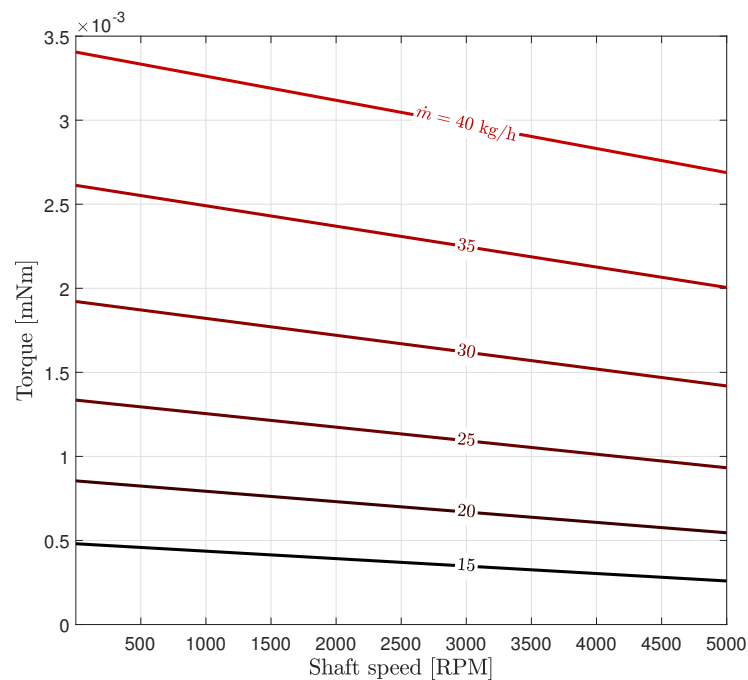
A virtual prototype of the turbine was developed using the analytical method proposed by Guha and Sengupta [79] and conservation laws for modelling the inlet plenum chamber. When providing the dimensions of the turbine and the operating conditions (inlet mass flow rate and rotor shaft speed) as inputs, the virtual prototype model outputs the theoretical torque and power production. This proposed model is purposefully optimal, i.e., it provides an upper boundary for torque and power, disregarding frictional losses in the inlet tubes, plenum chamber, bearings, and minor losses throughout the turbine, such as fluid leakage.

To simplify the validation of the turbine, the rotor and plenum chamber diameters were chosen as 50 mm and 100 mm, respectively, consistent with the validated turbine design developed by Lemma et al. [88].
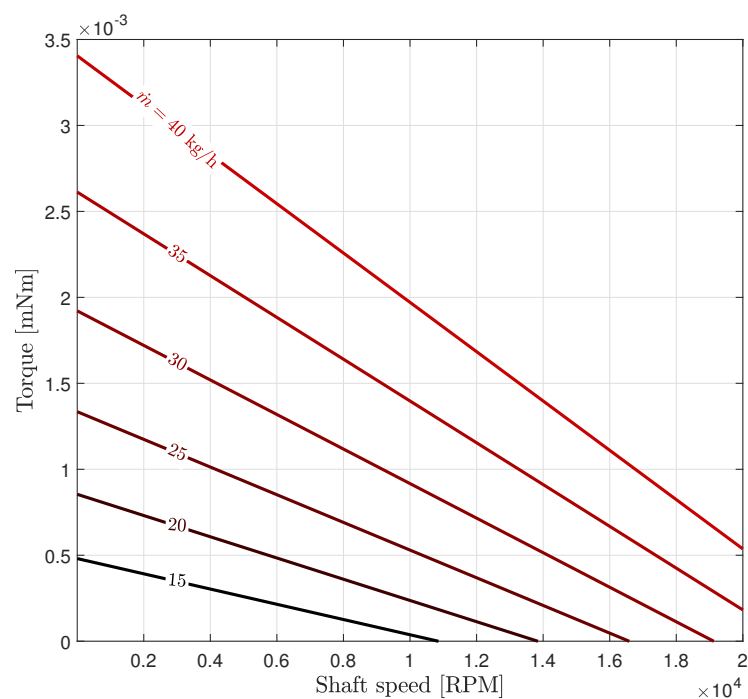
For the expected operating conditions, the mass flow rate was determined by the maximum value of peak expiratory flow rate for children, as this would represent a lower bound for use in prosthetics. The values were taken as 40 kg/h (approximately 550 Ls/min with saturated air at 100 % relative humidity and a body temperature of 37 °C, 1 atm—$\rho = 1.1147$ kg/m^3, $\mu = 1.8347 \times 10^{-5}$ Ns/m^2) [99,100], while the order of magnitude of the maximum shaft speed that could be generated by breathing was assessed by a pilot study as 1883 rotations per minute (RPM) ($n = 13$, 99.9 % confidence).

The aforementioned design values were fed into our virtual prototype model. A disc gap was chosen to maximise the torque and, consequently, the power with respect to our inlet conditions, and later rounded to be 0.2 mm to aid in manufacturing. A height of

10 mm and 9 discs were chosen for the turbine. Figures 3 and 4 show the theoretical torque and power predicted by the virtual prototype model as a function of the shaft's speed and inlet mass flow rate.

(a)

(b)

Figure 3. Generated torque vs. shaft speed for several mass flow rates. (**a**) Shows the torque generated by a shaft speed of up to 5000 RPM. (**b**) Shows the torque generated by a shaft speed of up to to 20,000 RPM.
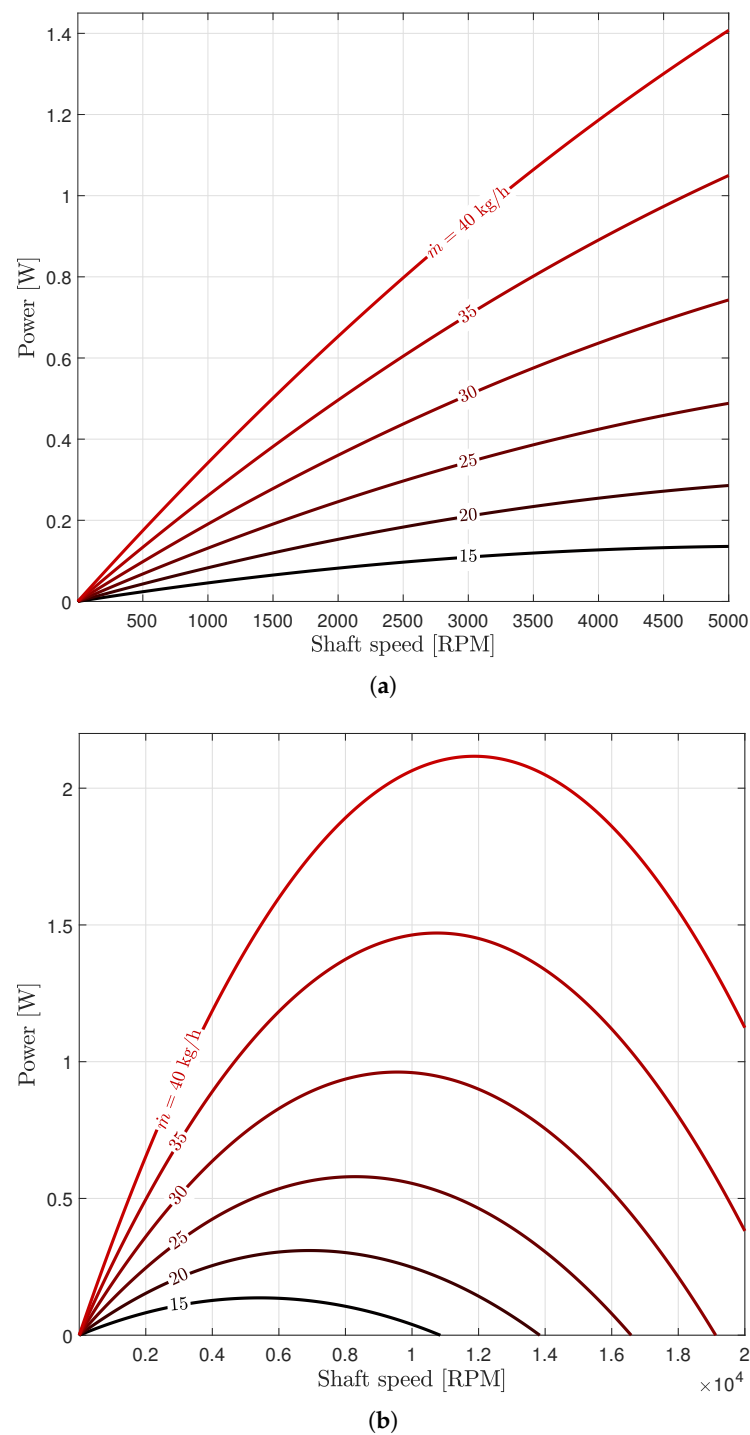
Figure 4. Generated power vs. shaft speed for several mass flow rates. (**a**) Shows the power generated by a shaft speed of up to 5000 RPM. (**b**) Shows the torque generated by a shaft speed of up to to 20,000 RPM.

From Figures 3 and 4, it can be noted that there is a linear relationship between the turbine's torque and the shaft speed, which results in parabolic power production, as expected [79,88]. The torque is maximum at stall (0 RPM) and reaches zero at a given RPM, after which the turbine starts to behave as a compressor – needing a torque supply, consuming power, and increasing the fluid's pressure. Frictional bearing losses in the turbine would change the slope of the torque curves and translate the maximum power location [88]. For a given mass flow rate, there is a single maxima for the power curve. As

expected, the higher the mass flow rate through the turbine, the higher the overall power and torque produced.

In Section 3.1, we turn our attention to the shaft speeds lower than 5000 RPM, within our expected range of what a child could spin the turbine through breathing. Most of the power maxima lie outside of this range, which means that maximising the power would simply mean breathing in as much air as possible and letting the turbine spin as fast as possible. However, maximisation of torque requires lower speeds, as its maximum is at stall. This allows for another degree of freedom for the user when controlling the device, as the breathing level could affect closing time and grip force.

3.2. Transmission

After optimising the Tesla turbine's parameters, the outputs of this model were fed to a mathematical model of our transmission system (that was based on standard mechanical design calculations and practices) to achieve the desired size, torque, RPM, and power for finger actuation. The gearbox facilitated converting output from the turbine to a higher torque at a suitable lower RPM. The output of this optimised virtual transmission model was used to achieve the actuation of the TD. The modular transmission enables the Tesla turbine axis to be oriented along the dorsal/palmar aspect of the hand and thus facilitates geometric requirements. This modular gearbox (Figure 5) was designed as a series of meshing (simple and compound) spur gears and a worm drive at the last stage to ensure self-locking [98,101].
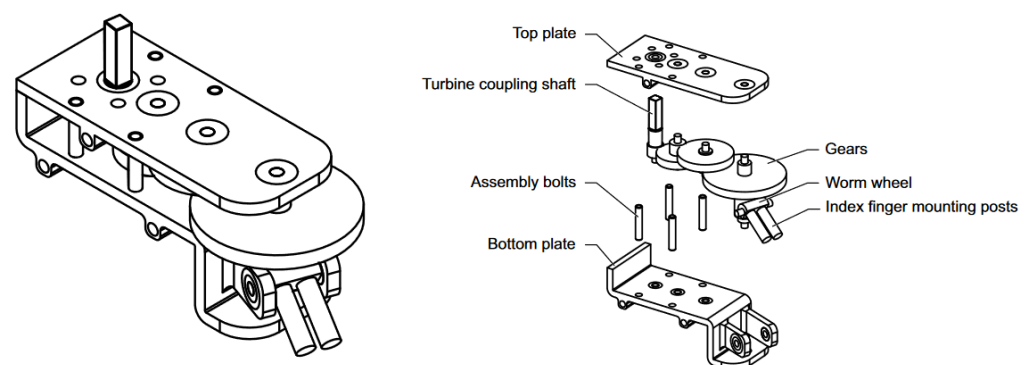

Figure 5. Schematic of the Modular Gearbox Design.

The worm gear at the final stage of the modular gearbox meshes with the truncated worm wheel at the base of the proximal phalanx of the index finger (i.e., along the metacarpophalangeal (MCP) joint axis) to actuate the index finger to close against the fixed thumb (Figure 5). The index finger, when opposed by the thumb, provides a cylindrical or tip grip based on the shape/size of the grasped object [102–104].

Two types of prehensors are typically utilised in BP prosthesis, consisting of voluntary opening (VO) or voluntary closing (VC), which for the traditional BP device is achieved when the Bowden cable is tensioned volitionally by the user [24,105,106]. Unfortunately, voluntary-opening BP prostheses are typically not feasible for young children [32]. However, the 'locking' ability of the breathing-powered prosthesis at any position and the ability to drive the system in both directions allows our device to be deemed as both VO and VC type. This enables the user to have a greater level of control than previously available with most BP devices. This is similar to a few prosthetic devices that offer the option of swapping between VO and VC mode (e.g., [107]).

Theoretically, this prosthesis can produce a grip force and response time [25] typical of active prostheses used by paediatric users. The gearbox helps transform the 2.5 Nmm at 2500 RPM input from the Tesla turbine rotor shaft to 1312 Nmm at 3.5 RPM output at the final stage for the TD actuation (with a total reduction of 720:1). To prevent slippage of the grasped object, the gripping force applied by the prosthesis user is adjusted to the

friction coefficient (μ) between the gripping surface (i.e., fingertips) and the object [103], which affects the shear force acting on the object. We have assumed a coefficient of friction of 0.5, corresponding to the rubber patches on the fingertip, for calculating the grip force in this study. An index finger length (when curled) of 6 cm and a range-of-motion of 70° were assumed to calculate the grip force and hand open/close time. This resulted in a theoretical value of 10.93 N (1.11 kg) of grip force and 3.36 s of response time. This 'Slow' version gearbox was used in user testing. Furthermore, we have designed another ('Fast') gearbox that transforms 2.5 Nmm at 2500 RPM input from the Tesla turbine rotor shaft to 409.9 Nmm at 11.1 RPM output at the final stage for the TD actuation (with a total reduction of 225:1). This results in a theoretical value of 3.42 N (0.35 kg) of grip force and 1.05 s of response time.

3.3. Demonstration—Preliminary User Testing

A demonstration model was produced based on the aforementioned design considerations to determine the feasibility of the proposed breathing-powered prosthetic concept. A 3D-printed modular design was created of the turbine, transmission, and anthropomorphic TD. Additive manufacturing was selected for several components (such as the turbine) as it has matured substantially in the last decade and now offers the potential to be integrated directly into the prosthetics field [108–111]. This utility of additive manufacturing is predominantly driven by the opportunity for personalisation, and the promise of improving device accessibility in low-resource settings [46,112].

The embodiment of the Tesla turbine underwent a considerable number of iterations during the development stage until a suitable manufacturing process was achieved. After this, a bespoke, modular, metallic gearbox was manufactured that was affixed to the 3D-printed anthropomorphic TD via fasteners. The 3D-printed index finger was rigidly attached to index finger mounting posts on the transmission. The transmission's input shaft attaches to the turbine rotor shaft via a square coupling. Silicone rubber patches were added at the tip of the thumb and index finger to achieve compliance and increase the coefficient of friction on the volar surface. The device is shown operational in Figure 6 by one of the paediatric volunteers. This model achieved successful TD opening and closing as well as grasping of an object by the child via breathing input. Supplementary user videos have been included that show the operational device. A silicon rubber tube is used, with one end attached to one of the turbine inlets and the other end connected to a nozzle, to allow for breathing input by the user. The self-locking aspect ensures the grasped object does not slip when the user stops breathing into the system.
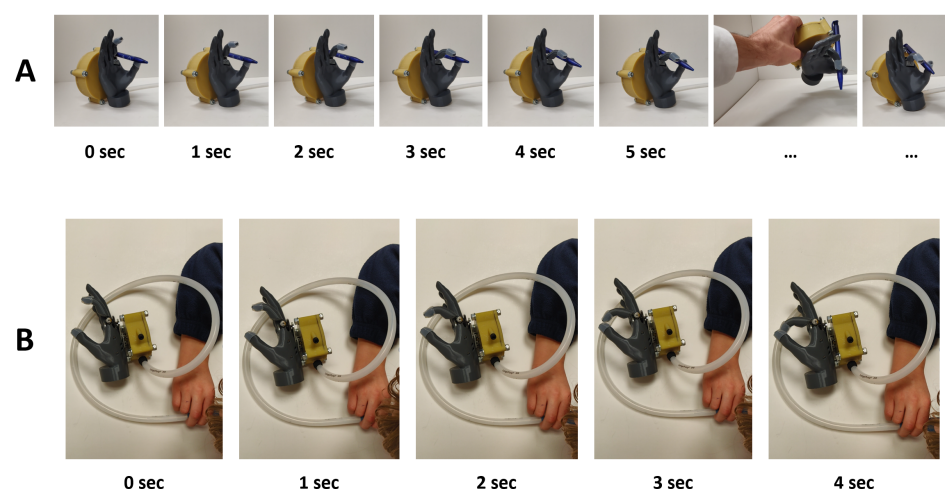

Figure 6. Demonstration model of breathing-powered prosthetic device. (**A**) Demonstration of the dynamic tip grip function with a pen. (**B**) Demonstration of the breathing-powered closing of the terminal device by a nine year-old volunteer.

4. Discussion

This is the first proof-of-concept study demonstrating the feasibility of a novel breathing-powered UL prosthesis. We used virtual prototyping to explore the design parameters and optimise the design before physical prototyping. Furthermore, the demonstration with a volunteer shows the potential functionality of the proposed concept. This novel way of powering and controlling the device allows it to compete with the traditional Bowden cable-driven BP devices while simultaneously overcoming several limitations of a cable-driven approach.

Most activities of daily living (ADLs) necessitate fast speed and low grip force (e.g., typing, gesturing) [25]. Tözeren suggests that a 0.8 s closing time is sufficient for prosthetic hands [95], although Dechev et al. [96] states a slightly slower 1.0–1.5 s closing time is adequate for conducting ADLs. The demonstration model has a relatively longer closing time, but minor changes to the gearbox can create the closing times suggested above. Ideally, a clutch-based gearbox could be developed in the future to provide the option to select between appropriate operation speed and grip strength delivery. This stage of development can and should be driven by further user input.

One of the main limitations of the current device is the lack of optimisation in extracting power from the turbine, while careful consideration was taken in the turbine's design to optimise its performance, there is still significant room for improvement. Further work should focus on building a suitable analytical/numerical model for the whole turbine assembly (rotor plus the inlet plenum chamber) validated by experimental investigations. Additionally, the experiments should ensure that there is proper control of the inlet mass flow rate and the shaft's speed, as current studies are limited by pressure control [88].

In addition, the manufacturing process of the rotor blades is reaching the edge of current machinery and conventional methods capabilities. Minimisation of the turbine's size and weight, as well as the maximisation of the turbine's power, relies on manufacturing very slender discs and spacers to a high precision – in this study, a 50 mm by 0.8 mm (diameter × height) disc with a 10 mm by 0.2 mm spacer for the gap were used. Further optimisation would need even thinner discs (to the order of 50 μm) while still keeping structural integrity under high centripetal loads.

The weight of the overall design is another important aspect that needs to be considered. The human hand on average weighs 400 g [113] or 0.6 % of the total body weight for men and 0.5 % for women [95]. Although, prosthetic TDs of an equivalent weight have been described as being 'too heavy' by users [15,40,114,115]. Since the forces from the prosthesis are borne by the soft tissue instead of the skeleton, the perceived weight of the TD is increased. Besides the overall device weight, the mass distribution affects the perceived weight of the system; hence, due consideration will be given to this aspect in the future. A range of 350–615 g is seen in current commercial prostheses and 350–2200 g in research-based hands [25]. Within the prosthetics field, no set specification exists for the maximum weight of the prosthesis; the only agreed-upon specification is to minimise weight in general [25]. The weight of the prosthetic device is a key contributor to socket interface discomfort and user fatigue. The prototype shown in the preliminary user testing weighs 429 g, with the wrist adaptor weighing 137 g. It should be noted that in this phase of the device development, the turbine is situated exterior to the TD, which adds mass to the overall system. This modular concept is useful for design exploration but should not be part of the final implementation. This study also used a gear module of 0.4 mm/teeth to reduce the transmission size. However, later we intend to explore a much smaller module in the order of 0.2–0.3 mm/teeth to help further miniaturise the transmission. Essentially, there will be a research interest in reducing the current gearbox's dimensions and weight.

In general, future work should focus on miniaturising the turbine and transmission to reduce the weight further. Ideally, the turbine will be integrated into the palm of the TD. This will directly reduce the weight of the overall system whilst also allowing for more aesthetically pleasing and anthropomorphic designs. In addition, future work could aim to use appropriate silicone gloves or conforming fingertip/palmar pads (i.e., friction pads on

the TD's volar surface to (i) increase the coefficient of friction and (ii) achieve compliance), which has been highly recommended in the mechanical design of prosthetic hands [25].

The use of 3D printing and associated manufacturing techniques for our device has been extremely vital to iterate across designs and achieve a working prototype in a cost-effective and timely manner. Nevertheless, additive manufacturing for creating prosthetics needs to be carefully considered, as 3D printed prosthetics are still lagging behind conventional prosthetics in terms of, e.g., clinical evidence [110]. Other manufacturing techniques should therefore be considered to scale the proposed system.

At the moment, the demonstration model has not been tested beyond the preliminary use of two volunteers. The volunteers were two boys aged nine and 11 who were asked to engage with the prototype without any acclimation time. The next steps will need to consist of validation of the device clinically by selecting (subjective and objective) outcome measures set within the WHO International Classification of Functioning, Disability, and Health (WHO-ICF) framework [116] and the recommendations by Upper Limb Prosthetic Outcome Measures (ULPOM) Group [117,118]. For example, the function can be tested by exploring the accuracy of patient's control of a TD, dexterity, grasp, and speed.

The lightweight tube used for input is stretchable, unlike the Bowden cable. This means that the user can look away without issues. Initial positive responses have been gathered with regards to the use of this approach from a small group of patient representatives. However, the mouthpiece does still need to be placed in the mouth for operation, and there are several ways in which this can be placed near the mouth for easy access. Further studies will be needed to explore the most appropriate design from a user perspective.

Another essential user consideration is the hygiene and sanitation of these kinds of devices. Users will need to be made aware that periodically cleaning the device might be required. Similar hygiene issues also exist in the control of motorised wheelchairs using the 'sip-and-puff' technology. This technology has been around for several decades and is also safely applied in other assistive technology. The application of appropriate valves will further help to ensure the safe use of these systems over time. These aspects will need to be explored in clinical user trials.

It should be noted that the device presented in this paper helps decouple aperture control from the control of the position of the prehensor in space. The presented design can open or close the hand without the need for contact or the requirement to hold/move a particular body part (e.g., shoulder) in a certain position.

Micera et al. [119] highlight that reliable and intuitive control of UL prostheses to obtain adequate dextrous manipulation requires sufficient feedback of prosthetic finger positions and pinch forces applied to objects. One of the problems with myoelectric devices is that they do not offer direct feedback of the forces or opening of the TD, as offered by a conventional harness and (Bowden) cable in BP prostheses. Although the absence of a harness is in some respects a great advantage of the myoelectric devices, the harness feedback ultimately enables the experienced user to feel the prehensor as a natural extension of their body.

Current BP prostheses offer the benefits of proprioceptive feedback [12], and it has been shown that this proprioceptive feedback is superior to visual and tactile feedback [120]. Conversely, a (myo)electric device requires its user to rely predominantly on visual feedback to estimate the end-effector position. However, auditory and tactile feedback from motor vibrations serves as a rough estimate of grasping forces, which is inferior to BP prostheses' proprioceptive feedback. It will be interesting to explore whether or not the breathing-powered device provides users with suitable feedback. Nevertheless, like an electric device, this device currently offers visual and auditory (in the form of noise from the gearbox and turbine rotor) feedback during device operation. However, understanding these aspects better, or perhaps, incorporating another feedback mechanism in the device [121–123] if required should be considered as future work.

Finally, it should be noted that the operation of the breathing-powered prosthesis does not seem to require any meaningful training time. There was no real acclimation

time given in the user demonstrations included in this paper. The volunteers came in and used the device straight "out of the box" without any practice. They were just asked to explore the device, while recordings were made of their interactions. The users were able to directly operate the device due to the comprehensive responsiveness to a simple, intuitive, and controllable input. Reducing or even (almost) eliminating training times will positively influence user acceptance rates and provide a valuable directionality for what can be achieved with novel prosthetic designs.

5. Conclusions

This study shows a demonstration of a novel BP prosthetic hand. This concept provides a step-change in how BP prostheses have been designed and offers new possibilities to those with a UL difference. It is one of the first truly new design approaches for power and control of BP prosthetics since the emergence of a cable-driven system over two centuries ago.

6. Patents

The authors are listed as co-inventors on a patent application (UK application no. 2113486.1) that covers the design and fabrication of the breathing-powered prosthetic system described in this manuscript.

Abbreviations

The following abbreviations are used in this manuscript:

ADL	Activity of daily living
BP	Body-powered (device)
CFD	Computational Fluid Dynamics
EP	Externally-powered (device)
MCP	Metacarpophalangeal (joint)
MSK	Musculoskeletal
NBDMs	Non-back-drivable mechanisms

QOL	Quality of life
RPM	Rotations per minute
TD	Terminal device
UE	Upper extremity
UL	Upper limb
VC	Voluntary closing
VO	Voluntary opening
ULPOM	Upper Limb Prosthetic Outcome Measures (Group)
WHO	World Health Organization
WHO—ICF	WHO—International Classification of Functioning, Disability, and Health

References

1. Stevens, P. Prosthetics in Resource-Limited Countries. *The O&P EDGE*, 2 June 2015.
2. WHO. United States Department of Defense, and MossRehab Amputee Rehabilitation Program. In *The Rehabilitation of People with Amputations*; World Health Organization: Geneva, Switzerland, 2004.
3. Bethge, M.; von Groote, P.; Giustini, A.; Gutenbrunner, C. The World Report on Disability: A challenge for rehabilitation medicine. *Am. J. Phys. Med. Rehabil.* **2014**, *93*, S4–S11. [CrossRef] [PubMed]
4. Ramamurthy, P.H. Enabling and caring for children with limb loss. *Paediatr. Child Health* **2021**, *31*, 347–351. [CrossRef]
5. Davids, J.R.; Wagner, L.V.; Meyer, L.C.; Blackhurst, D.W. Prosthetic management of children with unilateral congenital below-elbow deficiency. *J. Bone Jt. Surg.* **2006**, *88*, 1294–1300. [CrossRef]
6. Landsberger, S.; Shaperman, J.; Setoguchi, Y.; Fite, R.; Lin, A.; Vargas, V.; McNeal, D. Child prosthetic hand design: No small challenge. In Proceedings of the Wescon/96, Anaheim, CA, USA, 22–24 October 1996; IEEE: Piscataway, NJ, USA, 1996; pp. 236–240.
7. Hill, W.; Hermansson, L.M. Treatment for Children with Upper-Limb Differences in Various Parts of the World: Preliminary Findings. *JPO J. Prosthetics Orthot.* **2022**. [CrossRef]
8. Kuyper, M.A.; Breedijk, M.; Mulders, A.; Post, M.; Prevo, A. Prosthetic management of children in The Netherlands with upper limb deficiencies. *Prosthetics Orthot. Int.* **2001**, *25*, 228–234. [CrossRef]
9. Shaperman, J.; Landsberger, S.E.; Setoguchi, Y. Early upper limb prosthesis fitting: When and what do we fit. *JPO J. Prosthetics Orthot.* **2003**, *15*, 11–17. [CrossRef]
10. Krebs, D.E.; Edelstein, J.E.; Thornby, M.A. Prosthetic management of children with limb deficiencies. *Phys. Ther.* **1991**, *71*, 920–934. [CrossRef]
11. Hashim, N.A.; Abd Razak, N.A.; Abu Osman, N.A.; Gholizadeh, H. Improvement on upper limb body-powered prostheses (1921–2016): A systematic review. *Proc. Inst. Mech. Eng. Part H J. Eng. Med.* **2018**, *232*, 3–11. [CrossRef]
12. Simpson, D. The choice of control system for the multimovement prosthesis: Extended Physiological Proprioception (EPP). In *The Control of Upper-Extremity Prostheses and Orthoses*; Herberts, P., Kadefors, R., Magnusson, R., Petersen, I., Eds.; Charles C. Thomas: Springfield, IL, USA, 1974; pp. 146–150.
13. Henson, A. What Are My Prosthetic Options Based on My Amputation Level? 2021. Available online: https://www.armdynamics.com/upper-limb-library/what-are-my-prosthetic-options-based-on-my-amputation-level (accessed on 12 May 2021).
14. Gates, D.H.; Engdahl, S.M.; Davis, A. Recommendations for the Successful Implementation of Upper Limb Prosthetic Technology. *Hand Clin.* **2021**, *37*, 457–466. [CrossRef]
15. Biddiss, E.A.; Chau, T.T. Upper limb prosthesis use and abandonment: A survey of the last 25 years. *Prosthetics Orthot. Int.* **2007**, *31*, 236–257. [CrossRef] [PubMed]
16. Weir, R.; Sensinger, J.W.; Kutz, M. Design of artificial arms and hands for prosthetic applications. *Biomed. Eng. Des. Handb.* **2009**, *2*, 537–598.
17. Dorrance, D.W. Artificial Hand. U.S. Patent 1,042,413, 29 October 1912.
18. Zuo, K.J.; Olson, J.L. The evolution of functional hand replacement: From iron prostheses to hand transplantation. *Plast. Surg.* **2014**, *22*, 44–51. [CrossRef]
19. Childress, D.S. Historical aspects of powered limb prostheses. *Clin. Prosthetics Orthot.* **1985**, *9*, 2–13.
20. Borchardt, M.; Hartmann, K.; Leymann, R.; Schlesinger, S. *Limb Substitutes and Labour Assistive Devices for War Casualties and Traumatic Injured Persons [In German: Ersatzglieder und Arbeitshilfen: Für Kriegsbeschädigte und Unfallverletzte]*; Springer: Berlin, Germany, 1919; pp. 321–573.
21. Muilenburg, A.L.; LeBlanc, M.A. Body-powered upper-limb components. In *Comprehensive Management of the Upper-Limb Amputee*; Springer: Berlin/Heidelberg, Germany, 1989; pp. 28–38.
22. Meier, R.H. History of arm amputation, prosthetic restoration, and arm amputation rehabilitation. In *Functional Restoration of Adults and Children with Upper Extremity Amputation*; Demos Medical: New York, NY, USA, 2004; pp. 1–7.
23. Piazza, C.; Grioli, G.; Catalano, M.; Bicchi, A. A century of robotic hands. *Annu. Rev. Control. Robot. Auton. Syst.* **2019**, *2*, 1–32. [CrossRef]

24. Belter, J.T.; Reynolds, B.C.; Dollar, A.M. Grasp and force based taxonomy of split-hook prosthetic terminal devices. In Proceedings of the 2014 36th Annual International Conference of the IEEE Engineering in Medicine and Biology Society, Chicago, IL, USA, 26–30 August 2014; IEEE: Piscataway, NJ, USA, 2014; pp. 6613–6618.

25. Belter, J.T.; Segil, J.L.; SM, B. Mechanical design and performance specifications of anthropomorphic prosthetic hands: A review. *J. Rehabil. Res. Dev.* **2013**, *50*, 599. [CrossRef]

26. Chadwell, A.; Kenney, L.; Howard, D.; Ssekitoleko, R.T.; Nakandi, B.T.; Head, J. Evaluating reachable workspace and user control over prehensor aperture for a body-powered prosthesis. *IEEE Trans. Neural Syst. Rehabil. Eng.* **2020**, *28*, 2005–2014. [CrossRef]

27. Nagaraja, V.H.; Cheng, R.; Slater, D.H.; Thompson, M.S.; Bergmann, J.H. Upper-Limb Prosthetic Maintenance Data: A Retrospective Analysis Study. *JPO J. Prosthetics Orthot.* **2021**. [CrossRef]

28. Etter, K.; Borgia, M.; Resnik, L. Prescription and repair rates of prosthetic limbs in the VA healthcare system: Implications for national prosthetic parity. *Disabil. Rehabil. Assist. Technol.* **2015**, *10*, 493–500. [CrossRef]

29. Bhaskaranand, K.; Bhat, A.K.; Acharya, K.N. Prosthetic rehabilitation in traumatic upper limb amputees (An Indian perspective). *Arch. Orthop. Trauma Surg.* **2003**, *123*, 363–366. [CrossRef]

30. Pursley, R.J. Harness patterns for upper-extremity prostheses. *Artif. Limbs* **1955**, *2*, 26–60. [PubMed]

31. Kerver, N.; van Twillert, S.; Maas, B.; van der Sluis, C.K. User-relevant factors determining prosthesis choice in persons with major unilateral upper limb defects: A meta-synthesis of qualitative literature and focus group results. *PLoS ONE* **2020**, *15*, e0234342. [CrossRef] [PubMed]

32. Shaperman, J.; Leblanc, M.; Setoguchi, Y.; McNeal, D. Is body powered operation of upper limb prostheses feasible for young limb deficient children? *Prosthetics Orthot. Int.* **1995**, *19*, 165–175. [CrossRef] [PubMed]

33. Biddiss, E.; Beaton, D.; Chau, T. Consumer design priorities for upper limb prosthetics. *Disabil. Rehabil. Assist. Technol.* **2007**, *2*, 346–357. [CrossRef] [PubMed]

34. Smit, G.; Plettenburg, D.H. Efficiency of voluntary closing hand and hook prostheses. *Prosthetics Orthot. Int.* **2010**, *34*, 411–427. [CrossRef] [PubMed]

35. Smit, G.; Bongers, R.M.; Van der Sluis, C.K.; Plettenburg, D.H. Efficiency of voluntary opening hand and hook prosthetic devices: 24 years of development. *J. Rehabil. Res. Dev.* **2012**, *49*, 523–534. [CrossRef] [PubMed]

36. Hichert, M.; Vardy, A.N.; Plettenburg, D. Fatigue-free operation of most body-powered prostheses not feasible for majority of users with trans-radial deficiency. *Prosthetics Orthot. Int.* **2018**, *42*, 84–92. [CrossRef]

37. LeBlanc, M.; Setoguchi, Y.; Shaperman, J.; Carlson, L. Mechanical work efficiencies of body-powered prehensors for young children. *J. Assoc. Child.-Prosthet.-Orthotic Clin. JACPOC* **1992**, *27*, 70–75.

38. Hichert, M.; Abbink, D.A.; Kyberd, P.J.; Plettenburg, D.H. High cable forces deteriorate pinch force control in voluntary-closing body-powered prostheses. *PLoS ONE* **2017**, *12*, e0169996. [CrossRef]

39. Hichert, M.; Plettenburg, D.H. Ipsilateral Scapular Cutaneous Anchor System: An alternative for the harness in body-powered upper-limb prostheses. *Prosthetics Orthot. Int.* **2018**, *42*, 101–106. [CrossRef]

40. Biddiss, E.; Chau, T. Upper-limb prosthetics: Critical factors in device abandonment. *Am. J. Phys. Med. Rehabil.* **2007**, *86*, 977–987. [CrossRef] [PubMed]

41. Biddiss, E.; Chau, T. The roles of predisposing characteristics, established need, and enabling resources on upper extremity prosthesis use and abandonment. *Disabil. Rehabil. Assist. Technol.* **2007**, *2*, 71–84. [CrossRef] [PubMed]

42. Østlie, K.; Lesjø, I.M.; Franklin, R.J.; Garfelt, B.; Skjeldal, O.H.; Magnus, P. Prosthesis rejection in acquired major upper-limb amputees: A population-based survey. *Disabil. Rehabil. Assist. Technol.* **2012**, *7*, 294–303.

43. Cordella, F.; Ciancio, A.L.; Sacchetti, R.; Davalli, A.; Cutti, A.G.; Guglielmelli, E.; Zollo, L. Literature review on needs of upper limb prosthesis users. *Front. Neurosci.* **2016**, *10*, 209. [CrossRef] [PubMed]

44. Nagaraja, V.H.; Bergmann, J.H.; Sen, D.; Thompson, M.S. Examining the needs of affordable upper limb prosthetic users in India: A questionnaire-based survey. *Technol. Disabil.* **2016**, *28*, 101–110. [CrossRef]

45. Silcox, D., 3rd; Rooks, M.D.; Vogel, R.R.; Fleming, L.L. Myoelectric prostheses. A long-term follow-up and a study of the use of alternate prostheses. *J. Bone Jt. Surg. Am.* **1993**, *75*, 1781–1789. [CrossRef]

46. Farina, D.; Amsüss, S. Reflections on the present and future of upper limb prostheses. *Expert Rev. Med. Devices* **2016**, *13*, 321–324. [CrossRef] [PubMed]

47. Carey, S.L.; Lura, D.J.; Highsmith, M.J. Differences in myoelectric and body-powered upper-limb prostheses: Systematic literature review. *J. Rehabil. Res. Dev.* **2015**, *52*, 247–262. [CrossRef]

48. Salminger, S.; Stino, H.; Pichler, L.H.; Gstoettner, C.; Sturma, A.; Mayer, J.A.; Szivak, M.; Aszmann, O.C. Current rates of prosthetic usage in upper-limb amputees–have innovations had an impact on device acceptance? *Disabil. Rehabil.* **2020**, 1–12. [CrossRef]

49. Atkins, D.J.; Heard, D.C.; Donovan, W.H. Epidemiologic overview of individuals with upper-limb loss and their reported research priorities. *JPO J. Prosthetics Orthot.* **1996**, *8*, 2–11. [CrossRef]

50. LeBlanc, M.A. Innovation and improvement of body-powered arm prostheses: A first step. *Clin. Prosthetics Orthot.* **1985**, *9*, 13–16.

51. Engdahl, S.M.; Christie, B.P.; Kelly, B.; Davis, A.; Chestek, C.A.; Gates, D.H. Surveying the interest of individuals with upper limb loss in novel prosthetic control techniques. *J. Neuroeng. Rehabil.* **2015**, *12*, 1–11. [CrossRef] [PubMed]

52. Farina, D.; Vujaklija, I.; Brånemark, R.; Bull, A.M.; Dietl, H.; Graimann, B.; Hargrove, L.J.; Hoffmann, K.P.; Huang, H.H.; Ingvarsson, T.; et al. Toward higher-performance bionic limbs for wider clinical use. *Nat. Biomed. Eng.* **2021**, 1–13. [CrossRef] [PubMed]

53. Raspopovic, S.; Valle, G.; Petrini, F.M. Sensory feedback for limb prostheses in amputees. *Nat. Mater.* **2021**, *20*, 925–939. [CrossRef] [PubMed]

54. Raspopovic, S. Advancing limb neural prostheses. *Science* **2020**, *370*, 290–291. [CrossRef] [PubMed]

55. Ortiz-Catalan, M.; Mastinu, E.; Sassu, P.; Aszmann, O.; Brånemark, R. Self-contained neuromusculoskeletal arm prostheses. *N. Engl. J. Med.* **2020**, *382*, 1732–1738. [CrossRef]

56. Otte, A. Invasive versus Non-Invasive Neuroprosthetics of the Upper Limb: Which Way to Go? *Prosthesis* **2020**, *2*, 237–239. [CrossRef]

57. O'Brien, L.; Montesano, E.; Chadwell, A.; Kenney, L.; Smit, G. Real-world testing of the Self Grasping Hand, a novel adjustable passive prosthesis: A single group pilot study. *Prosthesis* **2022**, *4*, 48–59. [CrossRef]

58. Chadwell, A.; Chinn, N.; Kenney, L.; Karthaus, Z.J.; Mos, D.; Smit, G. An evaluation of contralateral hand involvement in the operation of the Delft Self-Grasping Hand, an adjustable passive prosthesis. *PLoS ONE* **2021**, *16*, e0252870. [CrossRef]

59. Plettenburg, D.H. Basic requirements for upper extremity prostheses: The WILMER approach. In Proceedings of the 20th Annual International Conference of the IEEE Engineering in Medicine and Biology Society. Vol. 20 Biomedical Engineering Towards the Year 2000 and Beyond (Cat. No. 98CH36286), Hong Kong, China, 1 November 1998; IEEE: Piscataway, NJ, USA, 1998; Volume 5, pp. 2276–2281.

60. Plettenburg, D.H. WILMER Elbow Control. 1999. Available online: https://www.tudelft.nl/3me/over/afdelingen/biomechanical-engineering/research/biomechatronics-human--machine-control/delft-institute-of-prosthetics-and-orthotics/products/prostheses/wilmer-elbow-control#:~:text=The%20WILMER%20elbow%20control%20is,of%20the%20elbow%20are%20used (accessed on 12 May 2022).

61. Kruit, J.; Cool, J. Body-powered hand prosthesis with low operating power for children. *J. Med. Eng. Technol.* **1989**, *13*, 129–133. [CrossRef]

62. Kenney, L.; Ssekitoleko, R.; Chadwell, A.; Donovan-Hall, M.; Morgado Ramirez, D.; Holloway, C.; Graham, P.; Cockroft, A.; Deere, B.; McCormack, S.; et al. *Prosthetics Services in Uganda: A Series of Studies to Inform the Design of a Low Cost, but Fit-for-Purpose, Body-Powered Prosthesis*; World Health Organization: Geneva, Switzerland, 2019.

63. Plettenburg, D. Upper limb prostheses—Future perspectives for body-powered prostheses. In Proceedings of the MEC Symposium Conference, Fredericton, NB, Canada, 10–13 August 2020.

64. Vujaklija, I.; Farina, D.; Aszmann, O.C. New developments in prosthetic arm systems. *Orthop. Res. Rev.* **2016**, *8*, 31. [CrossRef] [PubMed]

65. Taylor, C.R.; Srinivasan, S.S.; Yeon, S.H.; O'Donnell, M.K.; Roberts, T.J.; Herr, H.M. Magnetomicrometry. *Sci. Robot.* **2021**, *6*. [CrossRef] [PubMed]

66. Nazarpour, K. *Control of Prosthetic Hands: Challenges and Emerging Avenues*; Institution of Engineering and Technology: London, UK, 2020.

67. Basumatary, H.; Hazarika, S.M. State of the art in bionic hands. *IEEE Trans.-Hum.-Mach. Syst.* **2020**, *50*, 116–130. [CrossRef]

68. Russell, J.; Bergmann, J.H.; Nagaraja, V.H. Towards Dynamic Multi-Modal Intent Sensing Using Probabilistic Sensor Networks. *Sensors* **2022**, *22*, 2603. [CrossRef] [PubMed]

69. Controzzi, M.; Cipriani, C.; Carrozza, M.C. Design of artificial hands: A review. In *The Human Hand as an Inspiration for Robot Hand Development*; Springer Nature: Berlin/Heidelberg, Germany, 2014; pp. 219–246.

70. Plettenburg, D. Electric versus pneumatic power in hand prostheses for children. *J. Med. Eng. Technol.* **1989**, *13*, 124–128. [CrossRef]

71. Gu, G.; Zhang, N.; Xu, H.; Lin, S.; Yu, Y.; Chai, G.; Ge, L.; Yang, H.; Shao, Q.; Sheng, X.; et al. A soft neuroprosthetic hand providing simultaneous myoelectric control and tactile feedback. *Nat. Biomed. Eng.* **2021**, 1–10. [CrossRef]

72. Peterson, J.K.; Prigge, P. Early Upper-Limb Prosthetic Fitting and Brain Development: Considerations for Success. *JPO J. Prosthetics Orthot.* **2020**, *32*, 229–235. [CrossRef]

73. Borrell, J.A.; Copeland, C.; Lukaszek, J.L.; Fraser, K.; Zuniga, J.M. Use-Dependent Prosthesis Training Strengthens Contralateral Hemodynamic Brain Responses in a Young Adult With Upper Limb Reduction Deficiency: A Case Report. *Front. Neurosci.* **2021**, *15*, 693138. [CrossRef]

74. Copeland, C.; Mukherjee, M.; Wang, Y.; Fraser, K.; Zuniga, J.M. Changes in Sensorimotor Cortical Activation in Children Using Prostheses and Prosthetic Simulators. *Brain Sci.* **2021**, *11*, 991. [CrossRef]

75. Zuniga, J.M.; Pierce, J.E.; Copeland, C.; Cortes-Reyes, C.; Salazar, D.; Wang, Y.; Arun, K.; Huppert, T. Brain lateralization in children with upper-limb reduction deficiency. *J. Neuroeng. Rehabil.* **2021**, *18*, 1–14. [CrossRef]

76. Zuniga, J.M.; Dimitrios, K.; Peck, J.L.; Srivastava, R.; Pierce, J.E.; Dudley, D.R.; Salazar, D.A.; Young, K.J.; Knarr, B.A. Coactivation index of children with congenital upper limb reduction deficiencies before and after using a wrist-driven 3D printed partial hand prosthesis. *J. Neuroeng. Rehabil.* **2018**, *15*, 1–11. [CrossRef] [PubMed]

77. Tesla, N. Turbine. U.S. Patent 1,061,206A, 6 May 1913.

78. Guha, A.; Smiley, B. Experiment and analysis for an improved design of the inlet and nozzle in Tesla disc turbines. *Proc. Inst. Mech. Eng. Part A J. Power Energy* **2010**, *224*, 261–277. [CrossRef]

79. Sengupta, S.; Guha, A. A theory of Tesla disc turbines. *Proc. Inst. Mech. Eng. Part A J. Power Energy* **2012**, *226*, 650–663. [CrossRef]

80. Pfenniger, A.; Vogel, R.; Koch, V.M.; Jonsson, M. Performance analysis of a miniature turbine generator for intracorporeal energy harvesting. *Artif. Organs* **2014**, *38*, E68–E81. [CrossRef]

81. Jonsson, M.; Zurbuchen, A.; Haeberlin, A.; Pfenniger, A.; Vogel, R. Vascular turbine powering a cardiac pacemaker: An in vivo case study. *Exp. Clin. Cardiol.* **2014**, *20*, 2000–2003.
82. Rice, W. Tesla Turbomachinery. In *Handbook of Turbomachinery*; Marcel Dekker: New York, NY, USA, 2003; pp. 861–874.
83. Rice, W. An analytical and experimental investigation of multiple-disk turbines. *J. Eng. Power* **1965**, *87*, 29–36. [CrossRef]
84. Armstrong, J.H. An Investigation of the Performance of a Modified Tesla Turbine. Master's Thesis, Georgia Institute of Technology, Atlanta, GA, USA, 1952.
85. Beans, E.W. Investigation into the performance characteristics of a friction turbine. *J. Spacecr. Rocket.* **1966**, *3*, 131–134. [CrossRef]
86. Hoya, G.; Guha, A. The design of a test rig and study of the performance and efficiency of a Tesla disc turbine. *Proc. Inst. Mech. Eng. Part A J. Power Energy* **2009**, *223*, 451–465. [CrossRef]
87. McGarey, S.; Monson, P. *Performance and Efficiency of Disk Turbines*; MEng Research Project Report No. 1203; Mathesis; University of Bristol: Bristol, UK, 2007.
88. Lemma, E.; Deam, R.; Toncich, D.; Collins, R. Characterisation of a small viscous flow turbine. *Exp. Therm. Fluid Sci.* **2008**, *33*, 96–105. [CrossRef]
89. Guha, A.; Sengupta, S. The fluid dynamics of the rotating flow in a Tesla disc turbine. *Eur. J. Mech.-B/Fluids* **2013**, *37*, 112–123. [CrossRef]
90. Matsch, L.; Rice, W. An asymptotic solution for laminar flow of an incompressible fluid between rotating disks. *J. Appl. Mech.* **1968**, *35*, 155–159. [CrossRef]
91. Schroeder, H.B. An Investigation of Viscosity Force in Air by Means of a Viscosity Turbine. Ph.D. Thesis, Rensselaer Polytechnic Institute, Troy, NY, USA, 1950.
92. Rice, W. An analytical and experimental investigation of multiple disk pumps and compressors. *J. Eng. Gas Turbines Power* **1963**, *85*, 191–198. [CrossRef]
93. Couto, H.; Duarte, J.; Bastos-Netto, D. The tesla turbine revisited. In Proceedings of the Eighth Asia-Pacific International Symposium on Combustion and Energy Utilization, Sochi, Russia, 10–12 October 2006.
94. Deam, R.; Lemma, E.; Mace, B.; Collins, R. On scaling down turbines to millimeter size. *J. Eng. Gas Turbines Power* **2008**, *130*. [CrossRef]
95. Tözeren, A. *Human Body Dynamics: Classical Mechanics and Human Movement*; Springer Science & Business Media: Berlin/Heidelberg, Germany, 1999.
96. Dechev, N.; Cleghorn, W.; Naumann, S. Multiple finger, passive adaptive grasp prosthetic hand. *Mech. Mach. Theory* **2001**, *36*, 1157–1173. [CrossRef]
97. Plooij, M.; Mathijssen, G.; Cherelle, P.; Lefeber, D.; Vanderborght, B. Lock your robot: A review of locking devices in robotics. *IEEE Robot. Autom. Mag.* **2015**, *22*, 106–117. [CrossRef]
98. Controzzi, M.; Cipriani, C.; Carrozza, M.C. Miniaturized non-back-drivable mechanism for robotic applications. *Mech. Mach. Theory* **2010**, *45*, 1395–1406. [CrossRef]
99. Paramesh, H. Normal peak expiratory flow rate in urban and rural children. *Indian J. Pediatr.* **2003**, *70*, 375–377. [CrossRef]
100. Swaminathan, S.; Venkatesan, P.; Mukunthan, R. Peak expiratory flow rate in south Indian children. *Indian Pediatr.* **1993**, *30*, 207–211.
101. Radzevich, S.P. *Dudley's Handbook of Practical Gear Design and Manufacture*; CRC Press: Boca Raton, FL, USA, 2016.
102. Keller, A.D.; Taylor, C.L.; Zahm, V. *Studies to Determine the Functional Requirements for Hand and Arm Prosthesis*; Department of Engineering University of California: Berkeley, CA, USA, 1947.
103. Heckathorne, C.W. Components for adult externally powered systems. In *Atlas of Limb Prosthetics, Surgical, Prosthetic, and Rehabilitation Principles*, 2nd ed.; Mosby-Year Book, Inc.: St. Louis, MI, USA, 1992; Chapter 6C, pp. 151–175.
104. Light, C.; Chappell, P.; Kyberd, P.; Ellis, B. A critical review of functionality assessment in natural and prosthetic hands. *Br. J. Occup. Ther.* **1999**, *62*, 7–12. [CrossRef]
105. Klopsteg, P.E.; Wilson, P.D. *Human Limbs and Their Substitutes*; Hafner: Sylvania, OH, USA, 1968.
106. LeBlanc, M. Use of prosthetic prehensors. *Prosthetics Orthot. Int.* **1988**, *12*, 152–154. [CrossRef]
107. Sensinger, J.W.; Lipsey, J.; Thomas, A.; Turner, K. Design and evaluation of voluntary opening and voluntary closing prosthetic terminal device. *J. Rehabil. Res. Dev.* **2015**, *52*, 63. [CrossRef] [PubMed]
108. Cabibihan, J.J.; Abubasha, M.K.; Thakor, N. A method for 3-d printing patient-specific prosthetic arms with high accuracy shape and size. *IEEE Access* **2018**, *6*, 25029–25039. [CrossRef]
109. ten Kate, J.; Smit, G.; Breedveld, P. 3D-printed upper limb prostheses: A review. *Disabil. Rehabil. Assist. Technol.* **2017**, *12*, 300–314. [CrossRef] [PubMed]
110. Diment, L.E.; Thompson, M.S.; Bergmann, J.H. Three-dimensional printed upper-limb prostheses lack randomised controlled trials: A systematic review. *Prosthetics Orthot. Int.* **2018**, *42*, 7–13. [CrossRef] [PubMed]
111. Vujaklija, I.; Farina, D. 3D printed upper limb prosthetics. *Expert Rev. Med. Devices* **2018**, *15*, 505–512. [CrossRef]
112. Zuniga, J.M.; Young, K.J.; Peck, J.L.; Srivastava, R.; Pierce, J.E.; Dudley, D.R.; Salazar, D.A.; Bergmann, J. Remote fitting procedures for upper limb 3d printed prostheses. *Expert Rev. Med. Devices* **2019**, *16*, 257–266. [CrossRef] [PubMed]
113. Chandler, R.; Clauser, C.E.; McConville, J.T.; Reynolds, H.; Young, J.W. *Investigation of Inertial Properties of the Human Body*; Technical Report; Air Force Aerospace Medical Research Lab Wright-Patterson AFB: Dayton, OH, USA, 1975.

114. Pylatiuk, C.; Schulz, S.; Döderlein, L. Results of an Internet survey of myoelectric prosthetic hand users. *Prosthetics Orthot. Int.* **2007**, *31*, 362–370. [CrossRef]

115. Wagner, L.V.; Bagley, A.M.; James, M.A. Reasons for prosthetic rejection by children with unilateral congenital transverse forearm total deficiency. *JPO J. Prosthetics Orthot.* **2007**, *19*, 51–54. [CrossRef]

116. WHO. Towards a common language for functioning, disability, and health: ICF. In *The International Classification of Functioning, Disability and Health*; WHO: Geneva, Switzerland, 2002.

117. Hill, W.; Stavdahl, Ø.; Hermansson, L.N.; Kyberd, P.; Swanson, S.; Hubbard, S. Functional outcomes in the WHO-ICF model: Establishment of the upper limb prosthetic outcome measures group. *JPO J. Prosthetics Orthot.* **2009**, *21*, 115–119. [CrossRef]

118. Hill, W.; Kyberd, P.; Hermansson, L.N.; Hubbard, S.; Stavdahl, Ø.; Swanson, S. Upper Limb Prosthetic Outcome Measures (ULPOM): A working group and their findings. *JPO J. Prosthetics Orthot.* **2009**, *21*, P69–P82. [CrossRef]

119. Micera, S.; Carpaneto, J.; Raspopovic, S. Control of hand prostheses using peripheral information. *IEEE Rev. Biomed. Eng.* **2010**, *3*, 48–68. [CrossRef] [PubMed]

120. Mugge, W.; Abbink, D.A.; Schouten, A.C.; Van Der Helm, F.C.; Arendzen, J.; Meskers, C.G. Force control in the absence of visual and tactile feedback. *Exp. Brain Res.* **2013**, *224*, 635–645. [CrossRef] [PubMed]

121. Schofield, J.S.; Evans, K.R.; Carey, J.P.; Hebert, J.S. Applications of sensory feedback in motorized upper extremity prosthesis: A review. *Expert Rev. Med. Devices* **2014**, *11*, 499–511. [CrossRef] [PubMed]

122. Sensinger, J.W.; Dosen, S. A review of sensory feedback in upper-limb prostheses from the perspective of human motor control. *Front. Neurosci.* **2020**, *14*, 345. [CrossRef] [PubMed]

123. Alshaibani, F.; Thompson, M.S.; Bergmann, J.H. Experimental Analysis of a Novel, Magnetic-Driven Tactile Feedback Device. *Prosthesis* **2020**, *2*, 25–38. [CrossRef]